GEORGIAN MEDICAL NEWS

ISSN 1512-0112

NO 6 (375) Июнь 2026

ТБИЛИСИ - NEW YORK

ЕЖЕМЕСЯЧНЫЙ НАУЧНЫЙ ЖУРНАЛ

Медицинские новости Грузии

საქართველოს სამედიცინო სიახლენი

GEORGIAN MEDICAL NEWS

Monthly Georgia-US joint scientific journal published both in electronic and paper formats of the Agency of Medical Information of the Georgian Association of Business Press. Published since 1994. Distributed in NIS, EU and USA.

GMN: Georgian Medical News is peer-reviewed, published monthly journal committed to promoting the science and art of medicine and the betterment of public health, published by the GMN Editorial Board since 1994. GMN carries original scientific articles on medicine, biology and pharmacy, which are of experimental, theoretical and practical character; publishes original research, reviews, commentaries, editorials, essays, medical news, and correspondence in English and Russian.

GMN is indexed in MEDLINE, SCOPUS, PubMed and VINITI Russian Academy of Sciences. The full text content is available through EBSCO databases.

GMN: Медицинские новости Грузии - ежемесячный рецензируемый научный журнал, издаётся Редакционной коллегией с 1994 года на русском и английском языках в целях поддержки медицинской науки и улучшения здравоохранения. В журнале публикуются оригинальные научные статьи в области медицины, биологии и фармации, статьи обзорного характера, научные сообщения, новости медицины и здравоохранения. Журнал индексируется в MEDLINE, отражён в базе данных SCOPUS, PubMed и ВИНИТИ РАН. Полнотекстовые статьи журнала доступны через БД EBSCO.

GMN: Georgian Medical News – საქართველოს სამედიცინო სიახლენი – არის ყოველთვიური სამეცნიერო სამედიცინო რეცენზირებადი ჟურნალი, გამოიცემა 1994 წლიდან, წარმოადგენს სარედაქციო კოლეგიისა და აშშ-ის მეცნიერების, განათლების, ინდუსტრიის, ხელოვნებისა და ბუნებისმეტყველების საერთაშორისო აკადემიის ერთობლივ გამოცემას. GMN-ში რუსულ და ინგლისურ ენებზე ქვეყნდება ექსპერიმენტული, თეორიული და პრაქტიკული ხასიათის ორიგინალური სამეცნიერო სტატიები მედიცინის, ბიოლოგიისა და ფარმაციის სფეროში, მიმოხილვითი ხასიათის სტატიები.

ჟურნალი ინდექსირებულია MEDLINE-ის საერთაშორისო სისტემაში, ასახულია SCOPUS-ის, PubMed-ის და ВИНИТИ РАН-ის მონაცემთა ბაზებში. სტატიების სრული ტექსტი ხელმისაწვდომია EBSCO-ს მონაცემთა ბაზებიდან.

WEBSITE

www.geomednews.com

К СВЕДЕНИЮ АВТОРОВ!

При направлении статьи в редакцию необходимо соблюдать следующие правила:

1. Статья должна быть представлена в двух экземплярах, на русском или английском языках, напечатанная через **полтора интервала на одной стороне стандартного листа с шириной левого поля в три сантиметра**. Используемый компьютерный шрифт для текста на русском и английском языках - **Times New Roman** (**Кириллица**), для текста на грузинском языке следует использовать **AcadNusx.** Размер шрифта - **12**. К рукописи, напечатанной на компьютере, должен быть приложен CD со статьей.

2. Размер статьи должен быть не менее десяти и не более двадцати страниц машинописи, включая указатель литературы и резюме на английском, русском и грузинском языках.

3. В статье должны быть освещены актуальность данного материала, методы и результаты исследования и их обсуждение.

При представлении в печать научных экспериментальных работ авторы должны указывать вид и количество экспериментальных животных, применявшиеся методы обезболивания и усыпления (в ходе острых опытов).

4. К статье должны быть приложены краткое (на полстраницы) резюме на английском, русском и грузинском языках (включающее следующие разделы: цель исследования, материал и методы, результаты и заключение) и список ключевых слов (key words).

5. Таблицы необходимо представлять в печатной форме. Фотокопии не принимаются. **Все цифровые, итоговые и процентные данные в таблицах должны соответствовать таковым в тексте статьи**. Таблицы и графики должны быть озаглавлены.

6. Фотографии должны быть контрастными, фотокопии с рентгенограмм - в позитивном изображении. Рисунки, чертежи и диаграммы следует озаглавить, пронумеровать и вставить в соответствующее место текста **в tiff формате**.

В подписях к микрофотографиям следует указывать степень увеличения через окуляр или объектив и метод окраски или импрегнации срезов.

7. Фамилии отечественных авторов приводятся в оригинальной транскрипции.

8. При оформлении и направлении статей в журнал МНГ просим авторов соблюдать правила, изложенные в «Единых требованиях к рукописям, представляемым в биомедицинские журналы», принятых Международным комитетом редакторов медицинских журналов - http://www.spinesurgery.ru/files/publish.pdf и http://www.nlm.nih.gov/bsd/uniform_requirements.html
В конце каждой оригинальной статьи приводится библиографический список. В список литературы включаются все материалы, на которые имеются ссылки в тексте. Список составляется в алфавитном порядке и нумеруется. Литературный источник приводится на языке оригинала. В списке литературы сначала приводятся работы, написанные знаками грузинского алфавита, затем кириллицей и латиницей. Ссылки на цитируемые работы в тексте статьи даются в квадратных скобках в виде номера, соответствующего номеру данной работы в списке литературы. Большинство цитированных источников должны быть за последние 5-7 лет.

9. Для получения права на публикацию статья должна иметь от руководителя работы или учреждения визу и сопроводительное отношение, написанные или напечатанные на бланке и заверенные подписью и печатью.

10. В конце статьи должны быть подписи всех авторов, полностью приведены их фамилии, имена и отчества, указаны служебный и домашний номера телефонов и адреса или иные координаты. Количество авторов (соавторов) не должно превышать пяти человек.

11. Редакция оставляет за собой право сокращать и исправлять статьи. Корректура авторам не высылается, вся работа и сверка проводится по авторскому оригиналу.

12. Недопустимо направление в редакцию работ, представленных к печати в иных издательствах или опубликованных в других изданиях.

При нарушении указанных правил статьи не рассматриваются.

REQUIREMENTS

Please note, materials submitted to the Editorial Office Staff are supposed to meet the following requirements:

1. Articles must be provided with a double copy, in English or Russian languages and typed or compu-ter-printed on a single side of standard typing paper, with the left margin of **3** centimeters width, and **1.5** spacing between the lines, typeface - **Times New Roman** (**Cyrillic**), print size - **12** (referring to Georgian and Russian materials). With computer-printed texts please enclose a CD carrying the same file titled with Latin symbols.

2. Size of the article, including index and resume in English, Russian and Georgian languages must be at least 10 pages and not exceed the limit of 20 pages of typed or computer-printed text.

3. Submitted material must include a coverage of a topical subject, research methods, results, and review.

Authors of the scientific-research works must indicate the number of experimental biological species drawn in, list the employed methods of anesthetization and soporific means used during acute tests.

4. Articles must have a short (half page) abstract in English, Russian and Georgian (including the following sections: aim of study, material and methods, results and conclusions) and a list of key words.

5. Tables must be presented in an original typed or computer-printed form, instead of a photocopied version. **Numbers, totals, percentile data on the tables must coincide with those in the texts of the articles.** Tables and graphs must be headed.

6. Photographs are required to be contrasted and must be submitted with doubles. Please number each photograph with a pencil on its back, indicate author's name, title of the article (short version), and mark out its top and bottom parts. Drawings must be accurate, drafts and diagrams drawn in Indian ink (or black ink). Photocopies of the X-ray photographs must be presented in a positive image in **tiff format**.

Accurately numbered subtitles for each illustration must be listed on a separate sheet of paper. In the subtitles for the microphotographs please indicate the ocular and objective lens magnification power, method of coloring or impregnation of the microscopic sections (preparations).

7. Please indicate last names, first and middle initials of the native authors, present names and initials of the foreign authors in the transcription of the original language, enclose in parenthesis corresponding number under which the author is listed in the reference materials.

8. Please follow guidance offered to authors by The International Committee of Medical Journal Editors guidance in its Uniform Requirements for Manuscripts Submitted to Biomedical Journals publication available online at: http://www.nlm.nih.gov/bsd/uniform_requirements.html
http://www.icmje.org/urm_full.pdf
In GMN style for each work cited in the text, a bibliographic reference is given, and this is located at the end of the article under the title "References". All references cited in the text must be listed. The list of references should be arranged alphabetically and then numbered. References are numbered in the text [numbers in square brackets] and in the reference list and numbers are repeated throughout the text as needed. The bibliographic description is given in the language of publication (citations in Georgian script are followed by Cyrillic and Latin).

9. To obtain the rights of publication articles must be accompanied by a visa from the project instructor or the establishment, where the work has been performed, and a reference letter, both written or typed on a special signed form, certified by a stamp or a seal.

10. Articles must be signed by all of the authors at the end, and they must be provided with a list of full names, office and home phone numbers and addresses or other non-office locations where the authors could be reached. The number of the authors (co-authors) must not exceed the limit of 5 people.

11. Editorial Staff reserves the rights to cut down in size and correct the articles. Proof-sheets are not sent out to the authors. The entire editorial and collation work is performed according to the author's original text.

12. Sending in the works that have already been assigned to the press by other Editorial Staffs or have been printed by other publishers is not permissible.

Articles that Fail to Meet the Aforementioned Requirements are not Assigned to be Reviewed.

ავტორთა საყურადღებოდ!

რედაქციაში სტატიის წარმოდგენისას საჭიროა დავიცვათ შემდეგი წესები:

1. სტატია უნდა წარმოადგინოთ 2 ცალად, რუსულ ან ინგლისურ ენებზე,დაბეჭდილი სტანდარტული ფურცლის 1 გვერდზე, 3 სმ სიგანის მარცხენა ველისა და სტრიქონებს შორის 1,5 ინტერვალის დაცვით. გამოყენებული კომპიუტერული შრიფტი რუსულ და ინგლისურენოვან ტექსტებში - **Times New Roman (Кириллица)**, ხოლო ქართულენოვან ტექსტში საჭიროა გამოვიყენოთ **AcadNusx.** შრიფტის ზომა – 12. სტატიას თან უნდა ახლდეს CD სტატიით.

2. სტატიის მოცულობა არ უნდა შეადგენდეს 10 გვერდზე ნაკლებს და 20 გვერდზე მეტს ლიტერატურის სიის და რეზიუმეების (ინგლისურ, რუსულ და ქართულ ენებზე) ჩათვლით.

3. სტატიაში საჭიროა გაშუქდეს: საკითხის აქტუალობა; კვლევის მიზანი; საკვლევი მასალა და გამოყენებული მეთოდები; მიღებული შედეგები და მათი განსჯა. ექსპერიმენტული ხასიათის სტატიების წარმოდგენისას ავტორებმა უნდა მიუთითონ საექსპერიმენტო ცხოველების სახეობა და რაოდენობა; გაუტკივარებისა და დაძინების მეთოდები (მწვავე ცდების პირობებში).

4. სტატიას თან უნდა ახლდეს რეზიუმე ინგლისურ, რუსულ და ქართულ ენებზე არანაკლებ ნახევარი გვერდის მოცულობისა (სათაურის, ავტორების, დაწესებულების მითითებით და უნდა შეიცავდეს შემდეგ განყოფილებებს: მიზანი, მასალა და მეთოდები, შედეგები და დასკვნები; ტექსტუალური ნაწილი არ უნდა იყოს 15 სტრიქონზე ნაკლები) და საკვანძო სიტყვების ჩამონათვალი (key words).

5. ცხრილები საჭიროა წარმოადგინოთ ნაბეჭდი სახით. ყველა ციფრული, შემაჯამებელი და პროცენტული მონაცემები უნდა შეესაბამებოდეს ტექსტში მოყვანილს.

6. ფოტოსურათები უნდა იყოს კონტრასტული; სურათები, ნახაზები, დიაგრამები - დასათაურებული, დანომრილი და სათანადო ადგილას ჩასმული. რენტგენოგრამების ფოტოასლები წარმოადგინეთ პოზიტიური გამოსახულებით **tiff** ფორმატში. მიკროფოტოსურათების წარწერებში საჭიროა მიუთითოთ ოკულარის ან ობიექტივის საშუალებით გადიდების ხარისხი, ანათალების შეღებვის ან იმპრეგნაციის მეთოდი და აღნიშნოთ სურათის ზედა და ქვედა ნაწილები.

7. სამამულო ავტორების გვარები სტატიაში აღინიშნება ინიციალების თანდართვით, უცხოურისა – უცხოური ტრანსკრიპციით.

8. სტატიას თან უნდა ახლდეს ავტორის მიერ გამოყენებული სამამულო და უცხოური შრომების ბიბლიოგრაფიული სია (ბოლო 5-8 წლის სიღრმით). ანბანური წყობით წარმოდგენილ ბიბლიოგრაფიულ სიაში მიუთითეთ ჯერ სამამულო, შემდეგ უცხოელი ავტორები (გვარი, ინიციალები, სტატიის სათაური, ჟურნალის დასახელება, გამოცემის ადგილი, წელი, ჟურნალის №, პირველი და ბოლო გვერდები). მონოგრაფიის შემთხვევაში მიუთითეთ გამოცემის წელი, ადგილი და გვერდების საერთო რაოდენობა. ტექსტში კვადრატულ ფჩხილებში უნდა მიუთითოთ ავტორის შესაბამისი N ლიტერატურის სიის მიხედვით. მიზანშეწონილია, რომ ციტირებული წყაროების უმეტესი ნაწილი იყოს 5-6 წლის სიღრმის.

9. სტატიას თან უნდა ახლდეს: ა) დაწესებულების ან სამეცნიერო ხელმძღვანელის წარდგინება, დამოწმებული ხელმოწერითა და ბეჭდით; ბ) დარგის სპეციალისტის დამოწმებული რეცენზია, რომელშიც მითითებული იქნება საკითხის აქტუალობა, მასალის საკმაობა, მეთოდის სანდოობა, შედეგების სამეცნიერო-პრაქტიკული მნიშვნელობა.

10. სტატიის ბოლოს საჭიროა ყველა ავტორის ხელმოწერა, რომელთა რაოდენობა არ უნდა აღემატებოდეს 5-ს.

11. რედაქცია იტოვებს უფლებას შეასწოროს სტატია. ტექსტზე მუშაობა და შეჯერება ხდება საავტორო ორიგინალის მიხედვით.

12. დაუშვებელია რედაქციაში ისეთი სტატიის წარდგენა, რომელიც დასაბეჭდად წარდგენილი იყო სხვა რედაქციაში ან გამოქვეყნებული იყო სხვა გამოცემებში.

აღნიშნული წესების დარღვევის შემთხვევაში სტატიები არ განიხილება.

GEORGIAN MEDICAL NEWS
NO 6 (375) 2026

Содержание:

GEORGIAN MEDICAL NEWS
No 6 (375) 2026

ASSESSMENT OF VITEX AGNUS-COSTES PLANT EXTRACT ON THE HEART OF MICE EXPOSED TO OXIDATIVE STRESS

Essmat J. Jamel[1], Ayoub Ali Hussein Al-bayti[2], Alaa E. Jamal[3], Asmaa E. Jamal[4].

[1]*College of Nursing Science, University of Kirkuk, Kirkuk, Iraq.*

[2]*College of Health and Medical Techniques-kirkuk, Northern Technical University, Iraq. https://orcid.org/0000-0003-3621-3369*

[3]*Bahçeşehir University International, Istanbul, Turkey.*

[4]*Kirkuk Teaching Hospital, Kirkuk Health Directorate, Kirkuk, Iraq.*

Abstract.

Myocardial injury is largely the result of oxidative stress, which alters the structure and function of the heart's cardiomyaceous and conduction cells. The purpose of this investigation is to determine the relative effects of Vitex agnus-castus, a plant that is known to contain anti-inflammatory and antioxidant properties, upon the histology of the hearts of mice exposed to oxidative stress. Histological examinations were performed on the cardiac tissues of experimental groups of mice that were subjected to oxidative stress, either with or without treatment with V. agnus-castus extract. Whereas oxidative stress alone caused cardiomyocyte swelling, interstitial expansion, loss of striation, Purkinje fiber degeneration, and early necrotic alterations, control groups showed normal architecture with maintained muscle striations and centrally placed nuclei. By preserving nuclear morphology, reducing cytoplasmic degeneration, and maintaining intercalated discs and striations, treatment with V. agnus-castus, on the other hand, lessened these changes, indicating reduction of both cellular and conduction system damage. These results are in line with recent observations that phytochemicals from V. agnus-castus stabilize cellular membranes and scavenge reactive oxygen species (ROS) to produce cardioprotective effects. In conclusion, V. agnus-castus supplementation considerably reduced the cardiac damage caused by oxidative stress in rats, indicating that it may be a natural cardioprotective agent and indicating the need for additional mechanistic and translational research.

Key words. Myocardial injury, oxidative stress, vitex agnus-costes.

Introduction.

Vitex agnus-castus L. (chaste tree) has a long history as a medicinal plant, particularly for women's reproductive health. Traditionally, it was associated with chastity and reducing sexual desire. Roman women used its aromatic leaves and seeds for this purpose, monks chewed or carried its berries—giving rise to the names "monk's pepper" and "monk's berry"—and Athenian women placed its scented leaves on their beds during the Thesmophoria festival. Beyond this reputation, it was used in European and North American folk medicine for menstrual disorders, infertility, premenstrual symptoms, acne, digestive problems, and mild sedation. Herbalists also valued it for promoting menstruation, supporting lactation, and easing uterine inflammation. Other traditions used it for flatulence, dropsy, splenic disorders, pain, poisoning, hysteria, epilepsy, and mental illness, although it never became a major remedy in Chinese, Indian, or Ayurvedic medicine [1].

The genus Vitex has drawn scientific attention as a potential source of natural antimicrobial agents, given that several species are extensively employed in traditional medicine for conditions that may involve infectious processes. Vitex agnus-castus, in particular, is documented in Brazilian traditional practices for oral diseases and is linked to antiseptic and antifungal activities, supporting the notion that Vitex species harbor bioactive constituents capable of inhibiting microbial growth. Experimental investigations have demonstrated in vitro antimicrobial activity of these medicinal plants against Bacillus subtilis, Escherichia coli, Klebsiella pneumoniae, Pseudomonas aeruginosa, and Staphylococcus aureus. Vitex agnus-castus L. and Vitex negundo L. have been the most extensively studied species, evaluating not only bacterial pathogens but also fungi such as Aspergillus niger and Candida albicans, viruses including HIV-1, and parasites such as Plasmodium falciparum. Natural products such as agnucastoside, negundol, negundoside, and vitegnoside have been identified in Vitex extracts, with antimicrobial activity demonstrated across a diverse array of microbial strains [2]. Additionally, Vitex agnus-castus has been reported to exert anticancer effects by triggering mitochondria-dependent apoptosis mediated by reactive oxygen species, promoting cell-cycle arrest, and reducing the invasive, migratory, and proliferative capacity of several cancer types, including breast, bladder, colon, lung, oral, and ovarian cancers. Its active compound, casticin, appears to interfere with multiple cancer-related signaling pathways, particularly MAPK, NF-κB, and PI3K/Akt, through regulation of key cellular proteins. Casticin also enhances ROS production by increasing Bax expression while reducing Bcl proteins, thereby favoring apoptosis. In addition, it suppresses cell-cycle progression by affecting cdc25c, cdc2, and cyclin B1. Experimental animal studies have further demonstrated the potential role of casticin in limiting tumor growth and reducing metastatic spread in mouse models [3]

Vitex agnus-castus (VAC) and its constituent flavonoids, particularly casticin and vitexin, have a growing body of preclinical evidence supporting a mechanistic role in protecting the mammalian heart from oxidative stress-driven injury. However, there are still relatively few direct, well-standardized studies in mouse cardiac models, and many cardiocentric data come from rat models or noncardiac mouse tissues. It has been demonstrated that casticin preserves left-ventricular function and electrophysiological indices in ischemia–reperfusion (I/R) and chemically induced myocardial injury paradigms, reduces histological necrosis, lowers lipid peroxidation (malondialdehyde, MDA), and restores endogenous antioxidant

enzymes (superoxide dismutase, SOD; glutathione peroxidase, GPx) while simultaneously lowering proinflammatory cytokines (TNF-α, IL-1β, IL-6). These effects were documented in an I/R rat model and are consistent with attenuation of oxidative stress, inflammation, and apoptosis [4]. Mechanistically, casticin and vitexin share similarities along canonical redox-responsive signaling axes: they suppress NF-κB-driven proinflammatory/iNOS and COX-2 expression, upregulate the Nrf2/HO-1 cytoprotective program (with downstream increases in GSH and phase II antioxidant enzymes), and limit nitrative stress and blunt caspase-dependent cell death pathways (favorable Bax/Bcl-2 ratio, reduced cleaved caspase-3) [5]. The transcriptional mechanism that protects the myocardium against ischemia, anthracycline toxicity, and other ROS-mediated insults is regulated by Nrf2, which makes this a biologically viable pathway for VAC cardio protection [6]. Beyond heart-specific reports, systemic and tissue studies in mice show that VAC extracts reduce oxidative injury in cerebral ischemia models (permanent MCAO in ovariectomized mice) and exert estrogenic-like anti-inflammatory effects. This supports the translational relevance of anti-oxidative and anti-apoptotic actions across ischemic tissues and sexes [7]. Because mitochondrial ROS generation and permeability transition are upstream triggers for myocyte apoptosis and infarct expansion, VAC phytochemicals at the cellular level maintain mitochondrial ultrastructure and function in stressed myocardium in rodent models [4,5]. The observed improvements in contractile parameters and decreased arrhythmogenic changes in treated animals are likely due to VAC-associated reductions in MDA and ROS along with improved mitochondrial integrity. However, several disclaimers restrict instant translational claims; Numerous mouse-heart-specific endpoints (dose-response curves, pharmacokinetics, direct target engagement such as Nrf2 nuclear translocation in cardiomyocytes, and long-term functional outcomes after injury) are still poorly understood. Moreover, the phytochemical content and extract composition (cassicins, agnusides, and vitexin/isovitexin proportions) vary significantly by extraction method and plant source. Published cardiac studies also differ in model (I/R vs. isoproterenol vs. toxicant models), species (rat vs. mouse), dosing regimens, and timing (pre- vs. post-injury administration). All the aforementioned factors point to the likely effect of VAC and its flavonoids of providing a protective effect against oxidative stress to the heart - but further study on mice to determine the active ingredients of VAC and their effects on the heart is necessary to make firm findings regarding the effects of VAC on the hearts of mice [4,8].

So far further preclinical investigations are needed to clarify the pharmacokinetic profile of promising anticancer compounds, particularly the vitex agnus castus plant. Such studies could provide a stronger basis for evaluating its therapeutic potential and may support the future development of natural products as effective agents in cancer treatment. The current study aimed to investigate the effects of the aqueous extract of the agnus-castus plant on some functional characteristics of the heart of mice that were exposed to oxidative stress, as well as to investigate the interaction between the cardiovascular system and the vitex agnus castus plant in adult male rats.

Materials and Methods.

Collection of Plant Material and Preparation of Extracts: The fresh leaves of Vitex agnus-castus were collected from the College of Science, University of Baghdad by plant taxonomists. The collected leaves were air-dried under ambient settings, ground to a fine powder, and stored in plastic containers at ambient temperature (25°C) until extraction. 50 mg of powdered plant material was weighed and mixed with 5 mL of distilled water. The mixture was allowed to stand for 10 minutes at ambient temperature. The mixture was filtered through a 0.22 µm filter and the filtrate was concentrated in a water bath for 20 minutes. The crude aqueous extract was stored in glass vials at -20°C until required [8].

Dosage Optimization: In order to determine the appropriate dosage to be used in the treatment, a preliminary dose-response investigation was undertaken. Animals were randomly assigned to five groups (n=6 per group, with an equal number of male and female animals in each group) (Table 1). The following dosages were administered orally to each group of animals:

Group 1: 50 milligrams per kilogram of body weight
Group 2: 100 mg per kg of body weight
Group 3: 200 mg per kg of body weight
Group 4: 400 mg per kilogram of body weight
Group 5: 500 mg per kilogram of body weight

Blood samples were extracted from tail vein puncture after three hours of administration via capillary tubes. Serum was separated by centrifugation at 3,000 rpm for 5 min [9].

Laboratory Animals: This study used 120 healthy white albino mice (60 males and 60 females) aged between 12 and 16 weeks with a body weight of between 45 and 55 grams. Each animal was examined by a veterinarian to confirm that it was free of any diseases prior to the commencement of the experiment (Table 2). All animals were housed within sterile plastic enclosures that were sanitized daily over the 30 days of incubation.

Experimental Design.

Animals were allocated randomly into 10 groups (n=12 in each group, 6 males and 6 females):

1. **Control Group:** Standard water and diet for 30 days.
2. **Oxidative Stress Group:** 0.5% H_2O_2 in drinking water for 30 days.
3. **Plant Extract Group:** Aqueous plant extract (50 mg/kg b.w.) for 30 days.
4. **Extract + H_2O_2 Group:** Plant extract (50 mg/kg b.w.) combined with 0.5% H_2O_2 for 30 days.
5. **Extract + H_2O_2 + Vitamin E Group:** Plant extract (50 mg/kg b.w.) combined with 0.5% H_2O_2 and Vitamin E (100 mg/kg b.w.) for 30 days.
6. **Extract + Vitamin E Group:** Plant extract (50 mg/kg b.w.) combined with Vitamin E (100 mg/kg b.w.) for 30 days.
7. **High Extract + H_2O_2 Group:** Plant extract (100 mg/kg b.w.) combined with 0.5% H_2O_2 for 30 days.
8. **High Extract Group:** Plant extract (100 mg/kg b.w.) for 30 days.
9. **High Extract + H_2O_2 + Vitamin E Group:** Plant extract (100 mg/kg b.w.) combined with 0.5% H_2O_2 and Vitamin E (100 mg/kg b.w.) for 30 days.

10.**Vitamin E + H_2O_2 Group:** Vitamin E administration (100 mg/kg body weight) mixed with 0.5% hydrogen peroxide for 30 days.

Histological Processing: Following the period of decisive administration of the drug to the animals, the gastric tissues were excised and preserved in 10% neutral buffered formalin, and subjected to the procedures of conventional histology. The specimens were dehydrated in ethanol (70%, 80%, 90%, 100%), cleared in xylene, infused with molten paraffin wax, embedded in paraffin wax blocks, and sectioned into 4 µm sections with a rotary microtome. These sections were stained with hematoxylin and eosin (H&E) to enable histological examination of the tissue sections.

Microscopic Examination: The histological sections were analyzed with a light microscope (Optical S N 212973, Italy) integrated with a digital camera system (Digital Camera D C E-2) for photomicrographic documentation. Morphometric analysis was employed to evaluate the tissue sections.

Statistical analysis and morphometric assessments were carried out on the digitally recorded images to assess the changes in the histology of the samples from each group.

Results.

The histological slices of the heart tissue from the control group of mice stained with H&E are present in the light micrographs (panels a-c). The heart tissue from the control group of mice exhibits good condition in the heart tissue; the cardiomyocytes are present in bundles in a regular fashion with oval nuclei in the middle of each myocyte. Additionally, there is no necrosis, oedema, or inflammatory infiltrate in the myocardial tissue, indicating that the sarcoplasm of the heart tissue is intact. Furthermore, the interconnection of the cardiomyocytes is seen in the intercalated discs (seen in arrows in panel c) which is an essential feature of the heart in allowing for the myocardium to effectively contract. The tissue also appears to be devoid of any oxidative or ischemic damage since there are no nuclei that are pyknosis or vacuolization in the myocytes as well as no disrupted alignment of the myofibrils (Figure 1).

The light micrographs (panels a and b) that are displayed are of the control group's H&E-stained heart slices. Histological analysis reveals a well-organized myocardial architecture, with oval nuclei positioned in the center and longitudinally distributed heart muscle fibers with typical striations and undamaged cytoplasm. Uniform eosinophilia in the sarcoplasm and sparse intercellular gaps suggest that there is no oedema or interstitial inflammatory infiltration. Cardiomyocytes' structural and electrical connection is preserved, as evidenced by the intact appearance of intercalated discs (black arrows). Nuclear pyknosis, necrosis, vascular congestion, or cytoplasmic vacuolization are not seen. The mild fluctuations in the density of the fibers that occur occasionally (yellow arrows) are likely due to the sectioning of the myocardial tissue rather than to any pathogenic alterations to the tissue (Figure 2).

The control group's histological heart sections (panels a and b) stained with hematoxylin and eosin (H&E) show no pathological changes and normal myocardial architecture. Panel (a) displays intact myocardial (MC) and endocardium (EC), displaying compact and well-organized cardiac muscle fibers. As is typical of healthy cardiac tissue, the cardiomyocytes are elongated, striated, and organized in parallel bundles with oval nuclei in the center. The lack of presence of symptoms like oedema, congestion, or inflammatory infiltration is indicated by the small gaps between the cardiac fibers. Panels b) exhibit the effect of increased magnification of the cardiomyocytes, revealing the intact nuclei of the cells (yellow arrows) as well as the intercalated discs that connect the two muscle cells of the cardiomyocyte (black arrows). Furthermore, the symptoms of oxidative stress to the heart tissue are not present in these images, including the disruption of the myofibrils, the presence of vacuoles within the cytoplasm, pyknosis and necrosis of the nuclei of the cells (Figure 3).

Myocardial architectural changes are primarily reversible and just mildly visible in the photomicrograph. Only a small disruption of the ventricular wall's regular layering occurs at low power. While the intercalated discs are focally less defined (blurred) rather than entirely gone, the cardiomyocytes and Purkinje fibers look slightly enlarged (cellular cytoplasmic pallor and larger cell profile) at higher magnification. Nuclei that appear central in some cells (black arrows in b) and more peripheral in others (c) are examples of nuclear positioning discrepancies shown in the photos marked (b) and (c). Since cardiac myocytes typically have central nuclei, the "peripheral" appearance in some fields is probably due to local tissue distortion caused by swelling, sectioning/plane of section artefact, or admixture with changed conduction cells rather than myonuclear migration, which occurs spontaneously (Figure 4).

A slight disarray of cardiomyocyte bundles, slight increases in inter-myocyte cellularity (black arrows), and focal myocyte degenerative change with centrally located nuclei and preserved cross-striations (yellow arrows) are characteristics of the photomicrograph of group-5 (H&E, 100×–200×) that display a mild, focal disturbance of myocardial architecture. In contrast to established coagulative necrosis, these characteristics—cytoplasmic pallor/rarefaction with intact sarcomeric banding and only limited architectural loss—are more consistent with an early, low-grade (probably reversible) myocardial injury (intracellular edema/hydropic change or early degeneration) (Figure 5).

The H&E, 40×, 100×, and 200× light microscopic sections of Group 6 demonstrate a completely intact cardiac architecture with centrally located nuclei and a typical Purkinje fiber (PF) arrangement. While the cardiomyocytes' (CM) core nuclei and cross-striations are still there, the myofibrils appear somewhat stretched and wavy, and the interstitial spaces are noticeably wider. These slight alterations, in addition to mild cytoplasmic degeneration (yellow arrows), suggest that there is stress within the myocardial tissue leading to interstitial oedema, rather than the necrosis of the myofibers (Figure 6).

The H&E, 100X, and 200X light microscopy sections of group-7 exhibit some changes to the heart tissue in comparison to the normal morphology of the heart. The cardiomyocytes have their centrally-located nuclei (black arrows) indicating their normal structure, yet the Purkinje fibers (PF) and the cardiac fibers that contain those nuclei exhibit some degenerative changes (yellow arrows). The striations of the muscle fibers exhibit a slight decrease in strength indicating some disruption to the normal

Table 1. *Preliminary Dosage Optimization Design.*

Dose Optimization Group	Number of Animals	Sex Distribution	Treatment / Dose	Route	Sampling Time	Sample Collection
Group 1	6	Equal males and females	Plant extract, 50 mg/kg b.w.	Oral	3 hours after administration	Tail vein puncture
Group 2	6	Equal males and females	Plant extract, 100 mg/kg b.w.	Oral	3 hours after administration	Tail vein puncture
Group 3	6	Equal males and females	Plant extract, 200 mg/kg b.w.	Oral	3 hours after administration	Tail vein puncture
Group 4	6	Equal males and females	Plant extract, 400 mg/kg b.w.	Oral	3 hours after administration	Tail vein puncture
Group 5	6	Equal males and females	Plant extract, 500 mg/kg b.w.	Oral	3 hours after administration	Tail vein puncture

Table 2. *Main Experimental Design and Dosage Schedule.*

Group No.	Experimental Group	Number of Animals	Sex Distribution	Treatment	Dose / Concentration	Route / Administration	Duration
1	Control Group	12	6 males + 6 females	Standard diet and water	No treatment	Regular feeding and drinking water	30 days
2	Oxidative Stress Group	12	6 males + 6 females	Hydrogen peroxide only	0.5% H_2O_2	Drinking water	30 days
3	Plant Extract Group	12	6 males + 6 females	Aqueous plant extract only	50 mg/kg b.w.	Not specified	30 days
4	Extract + H_2O_2 Group	12	6 males + 6 females	Plant extract + hydrogen peroxide	Extract: 50 mg/kg b.w.; H_2O_2: 0.5%	Extract route not specified; H_2O_2 in drinking water	30 days
5	Extract + H_2O_2 + Vitamin E Group	12	6 males + 6 females	Plant extract + hydrogen peroxide + Vitamin E	Extract: 50 mg/kg b.w.; H_2O_2: 0.5%; Vitamin E: 100 mg/kg b.w.	Not fully specified	30 days
6	Extract + Vitamin E Group	12	6 males + 6 females	Plant extract + Vitamin E	Extract: 50 mg/kg b.w.; Vitamin E: 100 mg/kg b.w.	Not specified	30 days
7	High Extract + H_2O_2 Group	12	6 males + 6 females	High-dose plant extract + hydrogen peroxide	Extract: 100 mg/kg b.w.; H_2O_2: 0.5%	Extract route not specified; H_2O_2 in drinking water	30 days
8	High Extract Group	12	6 males + 6 females	High-dose plant extract only	100 mg/kg b.w.	Not specified	30 days
9	High Extract + H_2O_2 + Vitamin E Group	12	6 males + 6 females	High-dose plant extract + hydrogen peroxide + Vitamin E	Extract: 100 mg/kg b.w.; H_2O_2: 0.5%; Vitamin E: 100 mg/kg b.w.	Not fully specified	30 days
10	Vitamin E + H_2O_2 Group	12	6 males + 6 females	Vitamin E + hydrogen peroxide	Vitamin E: 100 mg/kg b.w.; H_2O_2: 0.5%	Vitamin E route not specified; H_2O_2 in drinking water	30 days

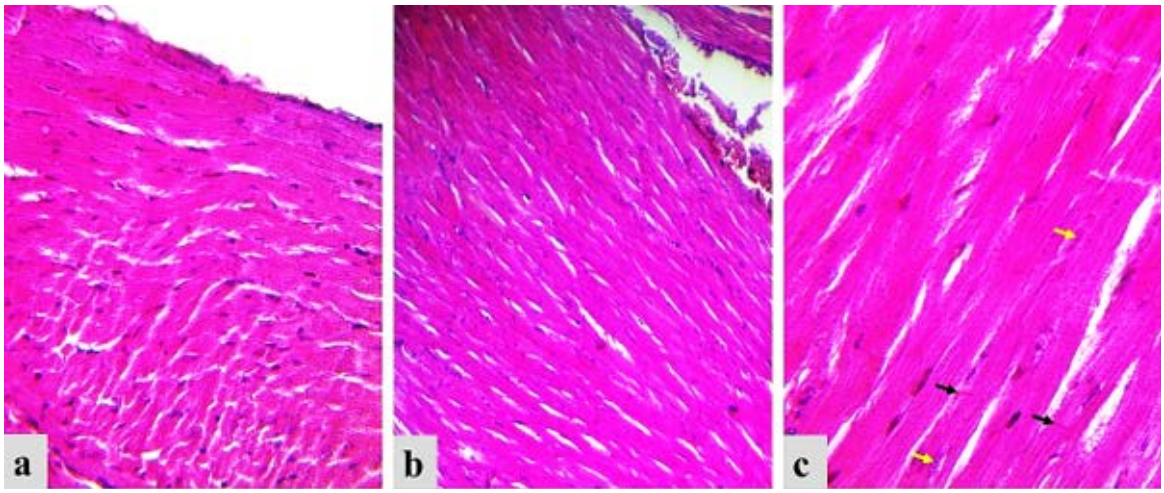

Figure 1. *A light microscopy of the control group's heart revealed the presence of the Purkinje fibre in (a), intercalated discs (black arrows) that connect the myocytes that have centrally located nuclei (yellow arrows) with normal muscle striation (H&E, 400X).*

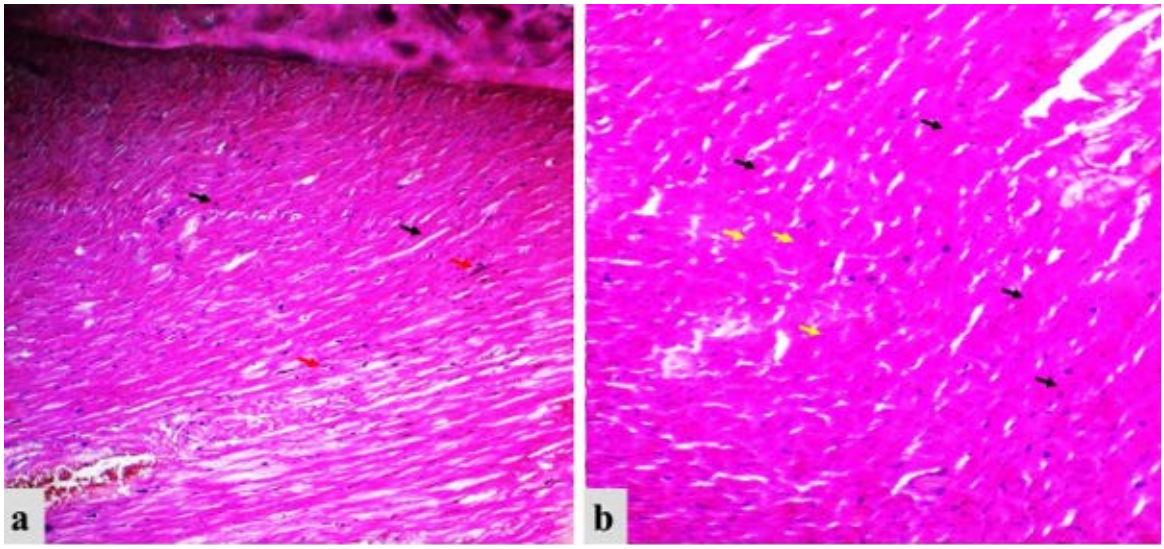

Figure 2. *The heart in group (2), a and b, has diffusely marked necrosis, loss of nuclei (yellow arrows), eosinophilic sarcoplasm in sub-endocardial regions, and mild cellularity among cardiomyocytes (red arrows). There is also marked myocardial degeneration with focal vacuolation of cardiomyocytes that showed internalizations of the large nuclei, and there is no muscle striation at all (H&E, 100X and 200X).*

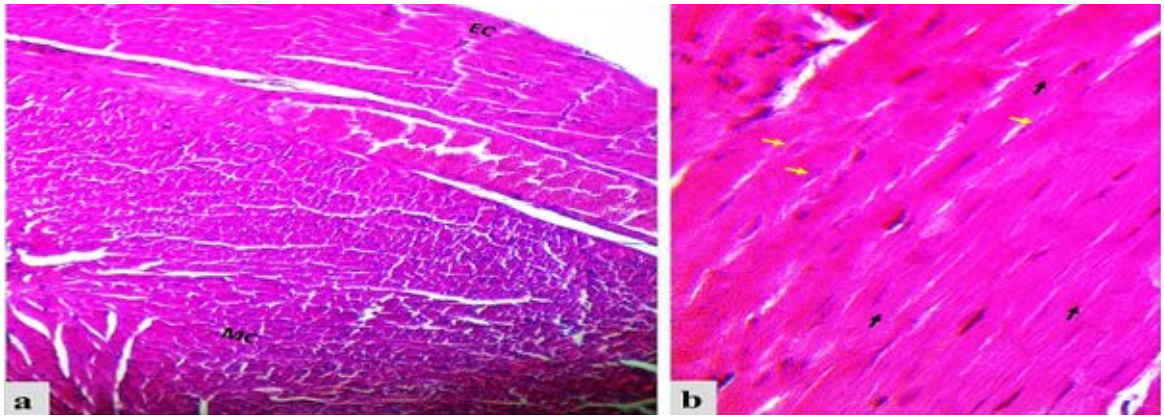

Figure 3. *The heart in group 3's light microscopic section revealed the following normal heart histological features: the striation of the cardiac muscle (black arrow), the presence of a Purkinje fiber in the endocardium (EC), the presence of myocytes in the myocardial layer (MC) that had a well-rounded oval shape, a different nucleolus (yellow arrows), and dispersed chromatin (H&E, 100X, and 400X).*

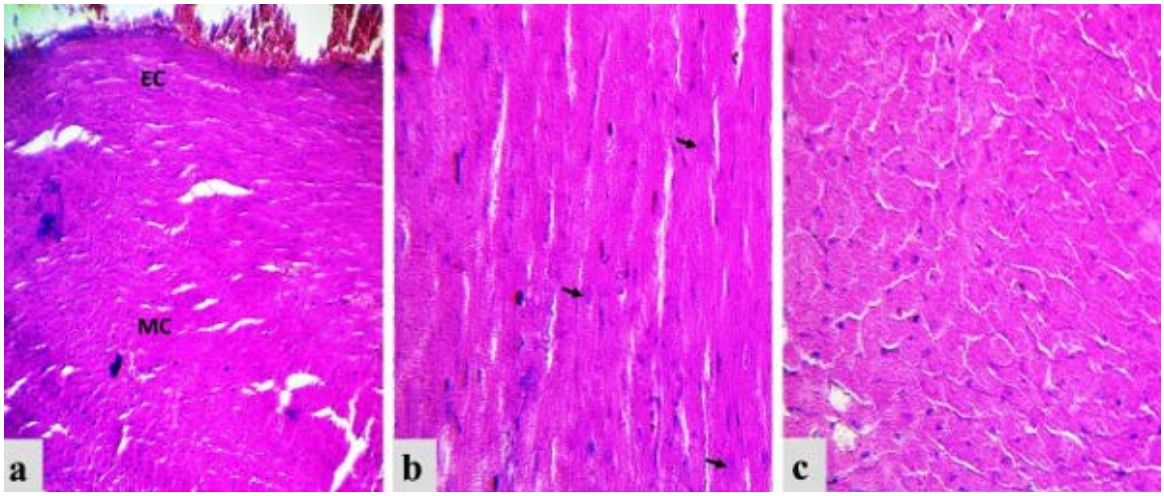

Figure 4. *The group 4 heart's light microscopic section is shown in a-c. Striation of muscle fibres was present, but intercalated discs were slightly blurred (H&E, 40X, 100X, and 400X). Purkinje fibres and cardiomyocytes displayed mild swelling with centrally located nuclei (black arrows in section b) and peripherally located nuclei in section (c).*

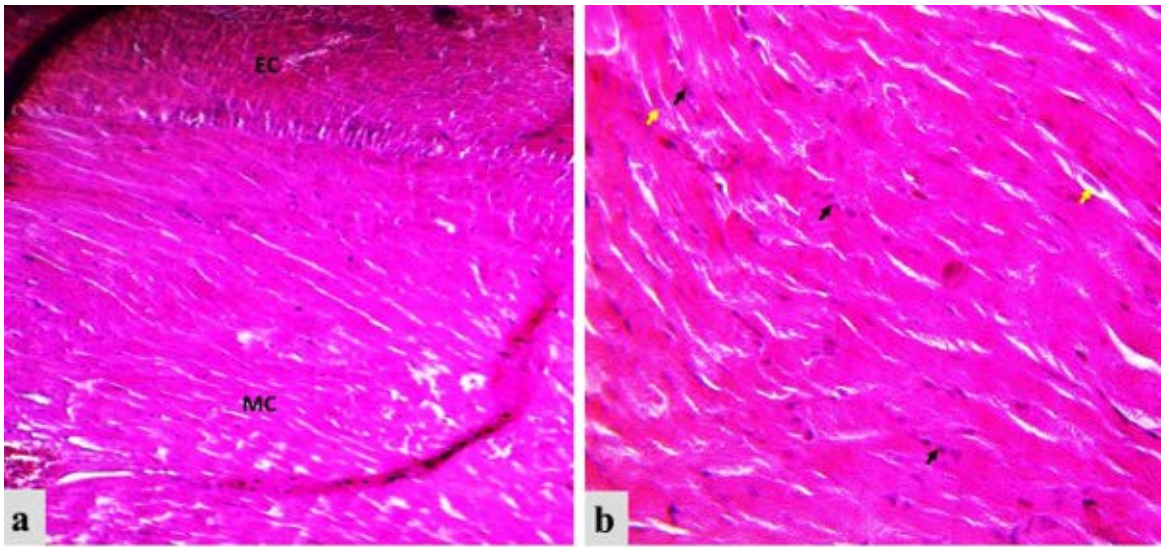

Figure 5. *Light microscopic section of group 5's heart shown in a and b: mild myocardial degeneration with centrally located nuclei (yellow arrows), mild cellularity among cardiomyocytes (black arrows), mild disruption in the organization of heart histology, and muscle striation still present (H&E, 100X and 200X).*

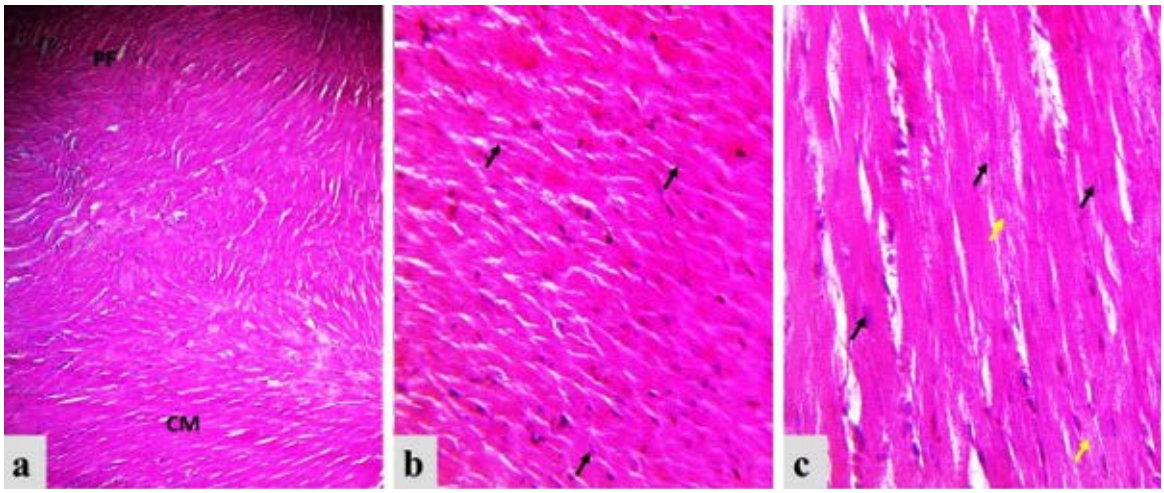

Figure 6. *A light microscopic section of group 6's heart is displayed in A-c. With nuclei in the middle and myofibrils that were stretched and wavy, the Purkinje fibers (PF) were placed normally. Although there was some degeneration in the interstitial spaces (CM) (yellow arrows), the nuclei stayed in the middle with intact muscle striation (H&E, 40X, 100X, and 200X).*

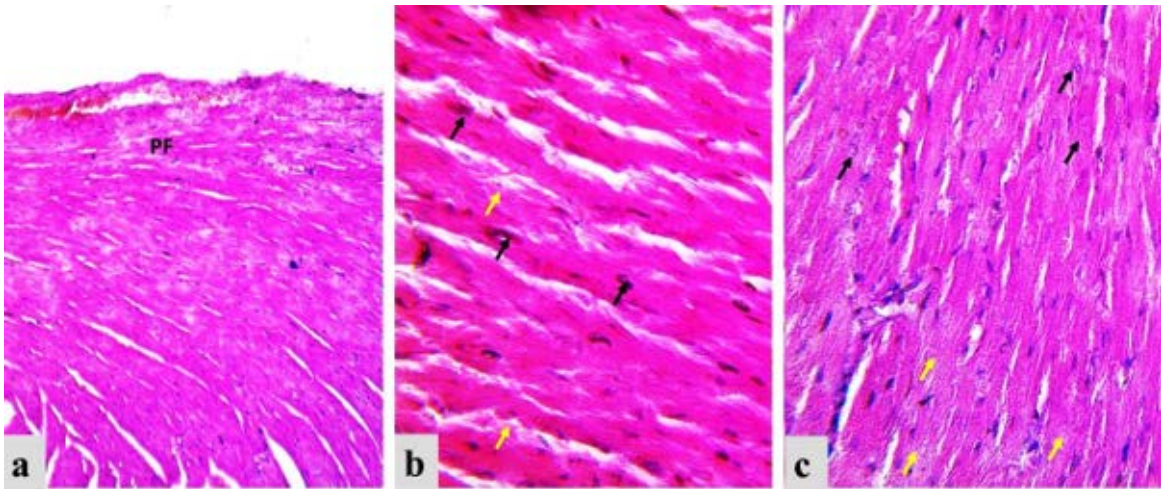

Figure 7. *Section of the heart under a light microscope in group 7a-c: The histological structures within the heart show some abnormalities. There is a loss of muscle striations (H&E, 100X, and 200X) and yellow arrows depict the Purkinje fibers (PF) and the cardiac fibers that contain the centrally-located nuclei (black arrows).*

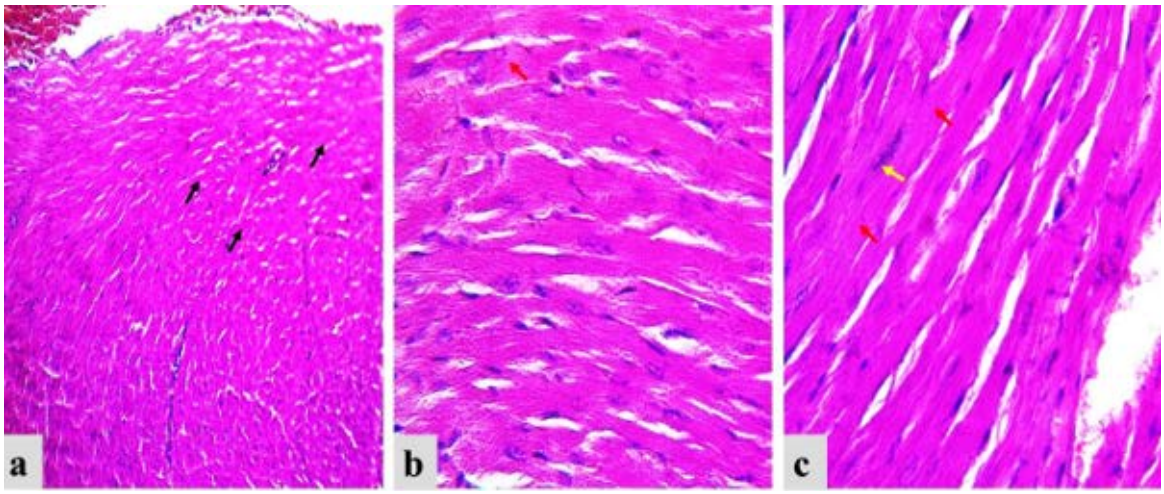

Figure 8. *Section of the heart under a light microscope in group 8a–c: The histological organization of the heart was mildly disturbed, with Purkinje fibers (PF) showing minor degeneration with centrally situated nuclei (yellow arrows), myofibrils appearing stretched and wavy, and certain interstitial spaces being expanded. According to H&E, 100X, and 400X, myocytes had lobulated, elongated nuclei with irregular, central chromatin clumps and a hardly perceptible nucleolus (black arrows) with a slight decrease of muscle striation.*

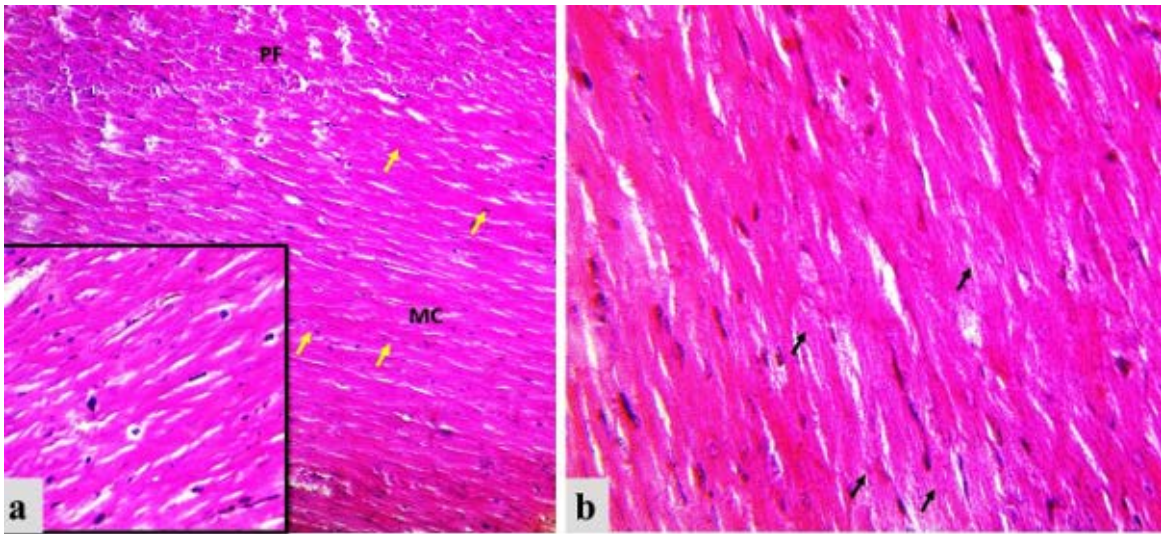

Figure 9. *Group 9's heart light microscopic sections, a and b: Mycoacaricides displayed mild-to-moderate necrosis, as evidenced by the loss of nuclei with eosinophilic sarcoplasm (yellow arrows and inset), mild-to-moderate degeneration of Purkinje fibers (PF) with centrally located nuclei, and also degeneration of myofibrils (black arrows) (H&E, 100X and 400X).*

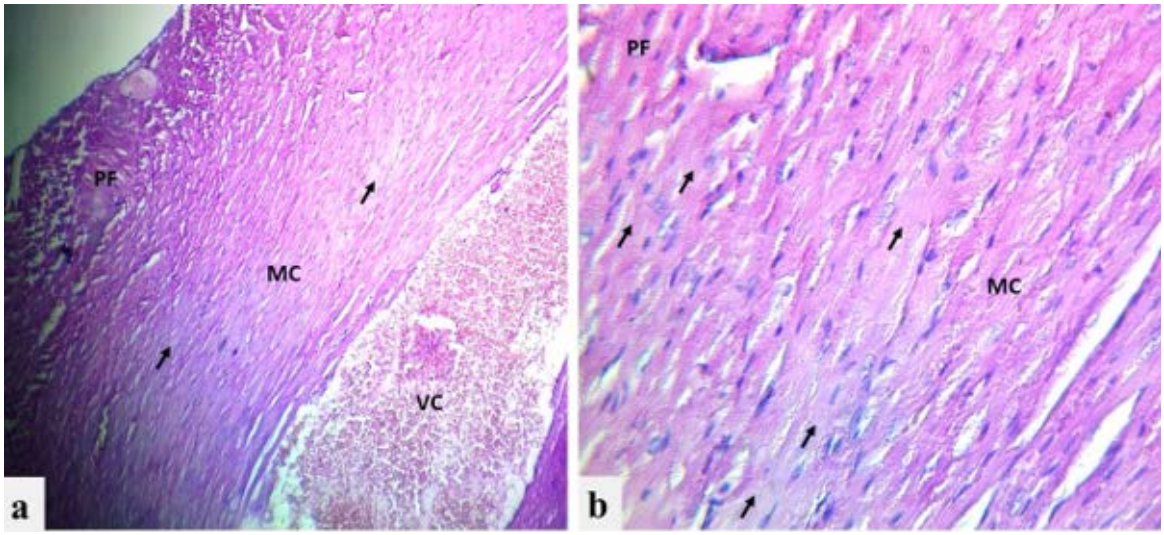

Figure 10. *The heart's light microscopic segment in group 10 was displayed in a and b. Black arrows that indicate the centrally placed nuclei, loss of intercalated discs, and mild-to-moderate loss of muscle striation indicate moderate Purkinje fiber (PF) and mycoacaricide (MC) degeneration (H&E, 100X and 400X).*

organization of the myofibrils of the heart muscle. However, there are no signs of necrosis within the cardiac tissue. Thus, the presence of degenerative changes to the Purkinje fibers and the loss of striations indicates the early stage of heart muscle injury, but the survival of the cardiomyocytes indicates that such an injury is not lethal (Figure 7).

Group-8's light microscopic sections (H&E, 100×, and 400×) show a little but noticeable disruption in the myocardium's typical histological arrangement. Purkinje fibres (PF) maintain their centrally placed nuclei (yellow arrows) despite exhibiting early degenerative alterations. Interstitial gaps are somewhat expanded, and the myofibrils seem stretched and wavy, suggesting early interstitial oedema. It is noteworthy that cardiomyocytes have lobulated, elongated nuclei with uneven chromatin clumping and poorly defined nucleoli (black arrows), which are indicative of early degenerative remodeling and nuclear atypia. There is also a little decrease in muscle striation, which indicates a partial disarray of the sarcomere architecture (Figure 8).

In comparison with the previous groups, the light microscopic sections of group 9 show more severe histopathological changes. Purkinje fibres exhibit mild to severe degenerative alterations, indicating susceptibility of the conduction system, but they are still identifiable due to their centrally situated nuclei. Cardiomyocytes display both necrotic and degenerative changes: several myocytes show mild to moderate necrosis with cytoplasmic eosinophilia, loss of structural detail, and nuclear loss (yellow arrows and inset), while myofibrils show degeneration (black arrows) (Figure 9).

The Purkinje fibers (PF) and cardiac fibers (MC) in the light microscopic segments of group 10 (H&E, 100×, and 400×) contain the centrally placed nuclei (black arrows) within the cardiomyocytes. However, there is a loss of the striations of the muscle cells. The loss of the intercalated discs is another noteworthy discovery in the photomicrographs. The intercellular discs in the heart's myocyte cells allow for the transmission of both mechanical and electrical force from one cardiomyocyte to the next (Figure 10).

Discussion.

The present study was designed to determine the effect of Vitex agnus-castus, a plant that is known to contain anti-inflammatory and antioxidant properties, upon the histology of the hearts of mice exposed to oxidative stress. The current study found that the heart tissue from the control group of mice exhibits good condition in the heart tissue devoid of any oxidative or ischemic damage. These characteristics of the heart tissue are similar to that described in previous research. For instance, Hassan and his colleagues described the architecture of healthy heart tissue from rats to be similar to that which is depicted in the images from the control group of mice, with intact myocardial fibers with centrally-located nuclei [10]. These same characteristics were also described by Muhammad, et al. in the hearts of control mice [11]. Furthermore, Arandhara et al. reported similar findings to those presented herein, stating that healthy hearts (as opposed to those subjected to oxidative stress or cardiotoxic substances) exhibit densely-packeted myofibrils along the length of the myocytes yet have no lytic or inflammatory material within the tissue [12]. These results, therefore, demonstrate the normal and intact structure of the heart tissue from the control group of mice, indicating that the hearts of the mice can be reliably utilized to determine whether certain treatments have a detrimental or beneficial impact upon the normal structure and function of the myocardium. Furthermore, the similarity of these results to those published in previous research confirms both the utility of these control groups of mice, as well as the reliability of their use in scientific publication. Moreover, from the image in Figure 2, it is apparent mild fluctuations in the density of the fibers that occur due to exposing to oxidative stress or cardiotoxic substances. These results confirm the structural and functional integrity of the control group's myocardial tissue, which is in line with the findings of previous research on normal heart tissue. Many scientists published research that confirmed the normal histoarchitecture of normal control rats tissue samples, noting that the hearts of untreated animals contain fibers that are intact and have no degenerative alterations within their cells [10]. Furthermore, control groups in studies of cardiotoxic agents have exhibited the same findings as those of Hassan, with intact and normal fibers within their myocardial tissue samples [11,12]. These healthy heart tissues can be utilized as a point of comparison to the hearts of experimental groups submitted to cardiotoxic drugs or stressors, whose tissues exhibit alterations like the presence of leukocytes, disintegrated cardiac fibers, vacuolization of the cardiac fiber's cytoplasm, and congestion of the myocardial tissue. Thus, these control groups' hearts provide an indication of the normal structural integrity of the myocardium, which can help to ensure the trustworthiness of the experimental group findings. The preservation of the heart tissue of control groups is thus indicative of the absence of oxidative or pathogenic stress within their samples, an indicator that is recognized as crucial to the assessment of the effects of such treatments, as indicated by current research.

As shown in group four, local tissue distortion caused by swelling, sectioning/plane of section artefact, or admixture with changed conduction cells rather than myonuclear migration, which occurs spontaneously. Moreover, the cardiomyocytes and Purkinje fibers are slightly enlarged and the cellular cytoplasmic pallor with larger cell profile at higher magnification. Comparison with recent research and interpretation: recovery on ultrastructural follow-up has been linked to mild cardiomyocyte swelling with preserved striations and reversible ultrastructural change, which is a well-known pattern in models of early/reversible myocardial injury (such as adrenergic injury, low-grade ischemia, or early toxic insult) [13]. While loss of sarcomere units and noticeable mitochondrial dense deposits suggest irreversible damage, electron-microscopy studies and experimental reports highlight that myocyte enlargement and streaming/clumping of myofilaments can be reversible [14]. Clinically, Purkinje fiber involvement is significant because even slight structural disruption of the conduction network (e.g., swelling, changes in glycogen, or junctional alteration) can promote arrhythmogenesis; Purkinje cells are known to be a substrate for ventricular arrhythmias when they are altered, despite their relative resistance to ischemia. The interpretation that your group-4 changes are consistent with an early or low-grade toxic/ischemic process rather than end-stage necrosis is

supported by a number of recent experimental cardiotoxicity studies (involving doxorubicin and other agents) that report an overlapping pattern: cytoplasmic pallor/hydropic change, focal loss/disruption of intercalated-disc components, and conduction-system vulnerability [15,16]. Lastly, work targeting intercalated-disc proteins (e.g., connexin-43, N-cadherin) demonstrates that mild disruption of these junctions can precede functional decline and is detectable histologically as blurring on H&E, and more clearly by immunostaining or EM [17]. This disruption or blurring of intercalated discs (gap junctions/desmosomes/adherent's complexes) has been highlighted as a mechanistic link between molecular stress and impaired electrical coupling. Useful suggestions and methods for enhancing the interpretation: To ascertain if the alterations are irreversible (mitochondrial dense deposits, sarcomere loss) or ultra-structurally reversible (swollen SR/mitochondria, myofilament streaming), conduct transmission electron microscopy (TEM) on representative samples. A junctional integrity, add immunohistochemistry for intercalated-disc proteins (connexin-43, N-cadherin, and desmoplakin) and use Masson's trichrome staining for fibrosis to rule out early replacement fibrosis. Since Purkinje involvement can have disproportionate electrophysiologic effects, connect histology with serum biomarkers (cTnT) and functional data (ECG, arrhythmia monitoring) if the experimental topic is cardiotoxicity [14,18]. Overall, group 4's sections exhibit mild, mostly reversible myocardial and Purkinje-system injury (cellular swelling with partial junctional blurring); this pattern is consistent with early/low-grade ischemic or toxic injury documented in recent experimental and review literature. The best way to determine severity and likely reversibility would be to conduct targeted ultrastructural and molecular follow-up (TEM, connexin-43/N-cadherin IHC, fibrosis stain, and functional correlation) [13].

It is interesting to note in the group five that slight disarray of cardiomyocyte bundles, slight increases in inter-myocyte cellularity (black arrows), and focal myocyte degenerative change with coagulative necrosis. This pattern is similar to descriptions of reversible cardiomyocyte injury in recent reviews of myocardial injury and troponin-positive but non-necrotic myocyte damage. Reactive interstitial cells or a mild inflammatory infiltrate (early/low-grade myocarditis) could be the cause of the slight increase in cellularity between fibers [19]. Since early inflammatory and toxic cardiomyopathies have been shown to exhibit similar focal cellular responses, immunophenotyping is necessary to differentiate lymphocytic inflammation from non-inflammatory reactive cells [20]. A typical alteration seen in preclinical cardiotoxicity models (such as anthracycline/doxorubicin damage), where early ultrastructural derangement comes before frank sarcomere loss and permanent myocyte death, is the preservation of cross-striations despite degeneration. Mechanistically, electrical instability can be predisposed by even minor structural disruptions that impair intercellular connection through connexin-43/intercalated-disc remodeling [15]. As advised by translational histopathology and biomarker studies of experimental cardiotoxicity, correlate these light-microscopic findings with targeted studies (Masson's trichrome for early fibrosis, TEM for ultrastructural reversibility, serum/functional markers like high-sensitivity troponin and ECG monitoring, and CD3/CD68 or CD45 IHC to phenotype interstitial cells) to elucidate pathogenesis and severity [15,21,22].

As mentioned in the result, the microscopic finding in group six demonstrate the myofibrils appear somewhat stretched and wavy, and the interstitial spaces are noticeably wider. In addition to mild cytoplasmic degeneration leading to interstitial oedema and the necrosis of the myofibers. These outcomes are in line with the past research that discovered that wavy myocardial fibers and increased interstitial spacing are indicators of strain placed upon the myocardium, which are features that are exhibited by individuals with either short-term or high-grade forms of ischemia. The presence of these features yet with preserved sarcomeres and nuclei indicates that these changes are likely adaptive and reversible in nature, supporting their classification as degenerative changes rather than changes indicative of cardiomyopathy [23,24]. According to recent research, the waviness of the myocardial fibers and the expansion of the interstitial space can be indicators of mechanical overload upon the heart. Additionally, these alterations to the normal structure of the myocardium can lead to the development of arrhythmias in those affected individuals due to the alterations to the proteins that compose Purkinje fibers and the intercalated discs. Furthermore, the severity of the changes in group-6 is less severe than that exhibited by individuals with anthracycline-induced cardiotoxicity, for example. Thus, these findings are similar to other studies that have recognized the early effects of myocardial strain. Overall, then, these findings suggest that group-6 displays only minor and potentially curable changes to the heart [25-27].

It is interesting to note that in the heart tissues for the group administered a high-extract plant with 0.5% H_2O_2 for 30 days showed the PF and the cardiac fibers that contain those nuclei exhibit some degenerative changes. The striations of the muscle fibers exhibit a decrease in strength indicating disruption to the normal organization of the myofibrils which indicates the early stage of heart muscle injury. Similar results, where wavy fibers, decreased striation, and conduction system involvement precede significant tissue necrosis, have been reported in experimental studies of early myocardial stress and cardiotoxicity [23,26]. According to observations on doxorubicin-induced cardiomyopathy models, reversible damage is also consistent with the preservation of central nuclei and mild myofibrillar changes. Significantly, even minor Purkinje fiber degradation has functional significance because recent research on Purkinje fiber susceptibility in stress-induced cardiomyopathy has shown that conduction system involvement, even at low levels, might predispose to arrhythmias [25,27]. The lesions seen in group-7 are rather modest in comparison to more advanced cardiotoxic damage, which is typified by myofibrillar disintegration and interstitial fibrosis. They resemble early adaptive responses that might heal if the stimulus is removed. Overall, the results point to early reversible cardiomyocyte injury, as shown by recent histological and translational studies, with partial loss of striation but retained nuclear morphology, as well as incipient myocardial and Purkinje fiber degeneration.

Another important finding was that the early interstitial oedema with lobulated cardiomyocytes and elongated nuclei

with uneven chromatin clumping and poorly defined nucleoli are found in the high extract group. These results allude to a pattern of stress-induced but not yet irreversible injury by indicating early degenerative cardiac alterations with both cytoplasmic and nuclear involvement [23,24]. Recent experimental and clinical research have documented similar characteristics, wherein oxidative stress or cardiotoxicity causes myocyte waviness, interstitial enlargement, nuclear abnormalities, and partial loss of cross-striations before necrosis and fibrosis develop [26]. Lobulation and chromatin clumping are two examples of nuclear abnormalities that have been identified as sensitive indicators of cardiac stress and are frequently linked to early apoptotic or degenerative events. Furthermore, Purkinje fiber involvement has clinical significance since, in models of structural and toxic cardiomyopathy, even minor damage to the conduction system has been associated with an increased risk of arrhythmogenesis [27]. The existence of nuclear abnormalities and partial loss of striations in group-8 indicates a development towards more advanced myocardial injury, albeit one that may be reversible if the underlying insult is addressed, in contrast to previous groups with less severe alterations [25]. Overall, these results show that nuclear atypia, interstitial expansion, and early conduction system involvement are indicative of mild but progressive myocardial degeneration in group-8 hearts. These findings are in line with the early stages of cardiotoxic or ischemic myocardial remodeling reported in recent studies.

Additionally, in comparison with the previous groups, the high extract+H_2O_2+Vitamin E group showed more severe histopathological changes. PF exhibit mild to severe degenerative alterations with mild to moderate necrosis of myocytes and loss of structural detail of the cytoplasm. Partially absent muscle striations provide additional evidence of myofibrillar dysfunction [23,24]. According to these results, there has been a shift from the reversible cellular stress observed in previous groups to more irreversible cardiac injury. The histological changes that indicate cardiomyocyte necrosis are present in both ischemic and drug-induced cardiomyopathies [26]. The changes from enlarged and wavy myocytes to loss of nuclei and myofibrils have been seen in models of doxorubicin and other cardiotoxic drugs [25,27]. The involvement of Purkinje fibers in these types of cardiomyopathies has been linked to the increased risk of arrhythmias due to the potential for degeneration of the conduction system. These findings are in line with current electrophysiological research on the topic. Furthermore, the necrotic characteristics in group 9 indicate irreversible damage to the myocytes, indicating advanced degeneration of the myocardium in comparison to the milder histological changes in groups 4-8.

The results, as shown in Figure 10, indicate more severe histopathological changes in the heart of mice of group ten due to administration 100 mg/kg Vitamin E with 0.5% H_2O_2 for 30 days. There is a loss of the striations of the muscle cells and the intercalated discs due to myocardial damage which is pathological responses in cardiotoxic and ischemic myocardial damage. The disruption can lead to myocardial damage and increased risk of conduction problems between the individual cardiac muscle cells. Connexin-43 downregulation and intercalated disc remodeling were found to be early pathological responses in cardiotoxic and ischemic myocardial damage, according to subsequent investigations that reported similar findings [25,27]. Since the integrity of the conduction system is necessary for a coordinated heart rhythm, the combination of mild Purkinje fiber degeneration and defective intercalated discs raises the possibility of both structural and electrophysiological repercussions. Additionally, cytoplasmic and junctional degeneration combined with partial nuclei preservation points to a more advanced but yet diverse state of damage, where both viable and degenerating myocytes coexist. Similar characteristics of myofibrillar degeneration, striation loss, and intercalated disc disruption are described by recent experimental cardiotoxicity models, such as those involving anthracyclines and oxidative stress, as precursors to irreversible cardiac remodeling and arrhythmogenesis [24,26]. Therefore, group 10's results show a moderate level of structural myocardial damage with intercellular uncoupling and conduction system involvement, which is quite similar to the intermediate-to-advanced degenerative phases of myocardial damage.

Conclusion.

One of the more significant findings to emerge from this study is that exposure to H_2O_2 caused clear cardiac tissue injury in the experimental mice, which mainly occur due to myocardial degeneration, reduced fibre striation, nuclear abnormalities, PF damage, and partial loss of intercalated disc integrity. Animals receiving aqueous V. agnus-castus extract provided better preservation of myocardial structure. The evidence from this study suggests a protective effect of V. agnus-castus against oxidative injury. This improvement may be linked to the plant's antioxidant and cytoprotective activity. Thus, V. agnus-castus appears to be a favourable natural cardioprotective agent; however, biochemical, molecular, and functional studies are still required to confirm its mechanisms and therapeutic relevance.

REFERENCES

1. Kamal N, Mio Asni NS, Rozlan INA, et al. Traditional Medicinal Uses, Phytochemistry, Biological Properties, and Health Applications of Vitex sp. Plants. 2022;11:1944.
2. Islam Z, Caldeira GI, Caniça M, et al. Vitex Genus as a Source of Antimicrobial Agents. Plants. 2024;13:401.
3. Ramchandani S, Naz I, Lee JH, et al. An Overview of the Potential Antineoplastic Effects of Casticin. Molecules. 2020;25:1287.
4. Ji L, Tian Z, Liu Y, et al. Protective effect of casticin in myocardial ischemia/reperfusion injury in rats via attenuation of oxidative stress and inflammation. Archives of Medical Science. 2021.
5. Liou C.-J, Cheng C-Y, Yeh K-W, et al. Protective Effects of Casticin from Vitex trifolia Alleviate Eosinophilic Airway Inflammation and Oxidative Stress in a Murine Asthma Model. Frontiers in Pharmacology. 2018;9:635.
6. Chen QM, Maltagliati AJ. Nrf2 at the Heart of Oxidative Stress and Cardiac Protection. Physiological Genomics. 2017;50.
7. Alimohamadi R, Fatemi I, Naderi S, et al. Protective effects of Vitex agnus-castus in ovariectomy mice following permanent middle cerebral artery occlusion. Iranian Journal of Basic Medical Sciences. 2019;22:1097-1101.

8. Özderin S. Determination of phenolic components of Vitex agnus-castus L. (Verbenaceae) from Muğla-Ula region in Turkey. Mustafa Kemal University Journal of Agricultural Sciences. 2021;26:692-699.
9. Al-Bajari S.A, Al-Akash M.A, Ismail H.K. Experimental detection of antioxidant and atherogenic effects of grapes seeds extracts in rabbits. Iraqi Journal of Veterinary Sciences. 2019;33:243-249.
10. Hassan M.Q, Akhtar M, Ahmed S, et al. Nigella sativa protects against isoproterenol-induced myocardial infarction by alleviating oxidative stress, biochemical alterations and histological damage. Asian Pacific Journal of Tropical Biomedicine. 2017;7:294-299.
11. Muhammad S, Akram M, Rasool G, et al. Cardioprotective Potential of Plant-Derived Molecules: A Scientific and Medicinal Approach. Dose-Response. 2019;27:1-14.
12. Arandhara A, Saha D, Das B.K. Evaluation of the cardioprotective potential of hydroethanolic extract of Koenigia polystachya L. (Qiú xù lião) leaves against isoproterenol-induced myocardial infarction in rats. Pharmacological Research - Modern Chinese Medicine. 2025;15:100612.
13. Nie J, George K, Duan F, et al. Histological evidence for reversible cardiomyocyte changes and serum cardiac troponin T elevation after exercise in rats. Physiological Reports. 2016;4:e13083.
14. Boyden P.A, Dun W, Robinson R.B. Cardiac Purkinje fibers and arrhythmias; The GK Moe Award Lecture 2015. Heart Rhythm. 2016;13:1172-1181.
15. Bhutani V, Varzideh F, Wilson S, et al. Doxorubicin-Induced Cardiotoxicity: A Comprehensive Update. Journal of Cardiovascular Development and Disease. 2025;12:242.
16. Shati A.A, A. Eid R, F. El-kott A, et al. Curcumin attenuates doxorubicin-induced cardiotoxicity via suppressing oxidative Stress, preventing inflammation and apoptosis: Ultrastructural and computational approaches. Heliyon. 2024;10:e27164.
17. Podyacheva E, Toropova Y. SIRT1 activation and its effect on intercalated disc proteins as a way to reduce doxorubicin cardiotoxicity. Front Pharmacol. 2022;13:1035387.
18. Canty J.M. Myocardial injury, troponin release, and cardiomyocyte death in brief ischemia, failure, and ventricular remodeling. American Journal of Physiology-Heart and Circulatory Physiology. 2022;323:H1-H15.
19. Li T, Yan Z, Fan Y, et al. Cardiac repair after myocardial infarction: A two-sided role of inflammation-mediated. Front Cardiovasc Med. 2022;9:1077290.
20. Sýkora M, Bacova BS, Andelova K, et al. Connexin43, A Promising Target to Reduce Cardiac Arrhythmia Burden in Pulmonary Arterial Hypertension. International Journal of Molecular Sciences. 2024;25:3275.
21. Pan D.-S, B. Li, Wang S.-L. Evaluation of biomarkers for doxorubicin-induced cardiac injury in rats. Exp Ther Med. 2022;24:712.
22. Sagris D, Georgiopoulos G, Pateras K, et al. Atrial High-Rate Episode Duration Thresholds and Thromboembolic Risk: A Systematic Review and Meta-Analysis. J Am Heart Assoc. 2021;10:e022487.
23. Espina-Jerez B, Aguiar-Frías AM, Siles-González J, et al. The Art of Childbirth of the Midwives of Al-Andalus: Social Assessment and Legal Implication of Health Assistance in the Cultural Diversity of the 10th-14th Centuries. Healthcare (Basel). 2023;11:2835.
24. Garcia-Vaquero M.L, Gama-Carvalho M, Pinto FR, et al. Biological interacting units identified in human protein networks reveal tissue-functional diversification and its impact on disease. Comput Struct Biotechnol J. 2022;20:3764-3778.
25. Prucha R, Hrubý V, Zaoralová D, et al. Coordination effects on the binding of late 3d single metal species to cyanographene. Phys Chem Chem Phys. 2022;25:286-296.
26. Wang K.W, Riveros I, DeLoye J, et al. Dynamic docking of small molecules targeting RNA CUG repeats causing myotonic dystrophy type 1. Biophys J. 2023;122:180-196.
27. Al-Azzawie A.F, Ajeel M.A, Al-Bayti A.A.H. Impact of gamma-aminobutyric acid receptors modulators on renal and liver functional, molecular and histological characteristics in white male mice. Reports of Morphology. 2024;30:82-92.